[13] S. Sadr and R. Adve, "Partially-distributed resource allocation in small-cell networks," *IEEE Trans. Wireless Commun.*, vol. 13, no. 12, pp. 6851–6862, Dec. 2014.

[14] E. Pateromichelakis, M. Shariat, A. Quddus, and R. Tafazolli, "Graph-based multicell scheduling in OFDMA-based small cell networks," *IEEE Access*, vol. 2, pp. 897–908, 2014.

[15] W. Ni and I. B. Collings, "A new adaptive small-cell architecture," *IEEE J. Sel. Areas Commun.*, vol. 31, no. 5, pp. 829–839, May 2013.

[16] "Further advancements for E-UTRA, physical layer aspects," Third-Generation Partnership Project, Sophia Antipolis Cedex, France, Tech. Rep. V9.0.0 36.814, Mar. 2010.

[17] " LTE in unlicensed spectrum: Harmonious coexistence with Wi-Fi," Qualcomm Res., San Diego, CA, USA, 2015.

[18] H. Zhang *et al.*, "Weighted sum-rate maximization in multi-cell networks via coordinated scheduling and discrete power control," *IEEE J. Sel. Areas Commun.*, vol. 29, no. 6, pp. 1214–1224, Jun. 2011.

[19] C. Tekin, M. Liu, R. Southwell, J. Huang, and S. Ahmad, "Atomic congestion games on graphs and their applications in networking," *IEEE/ACM Trans. Netw.*, vol. 20, no. 5, pp. 1541–1552, Oct. 2012.

[20] Y. Xu, Q. Wu, L. Shen, J. Wang, and A. Anpalagan, "Opportunistic spectrum access in cognitive radio networks: Global optimization using local interaction games," *IEEE J. Sel. Topics Signal Process.*, vol. 6, no. 2, pp. 180–194, Apr. 2012.

[21] Y. Xu, Q. Wu, L. Shen, J. Wang, and A. Anpalagan, "Opportunistic spectrum access with spatial reuse: Graphical game and uncoupled learning solutions," *IEEE Trans. Wireless Commun.*, vol. 12, no. 10, pp. 4814–4826, Oct. 2013.

[22] Y. Xu, Q. Wu, L. Shen, J. Wang, and A. Anpalagan, "Distributed channel selection in CRAHNs with heterogeneous spectrum opportunities: A local congestion game approach," *IEICE Trans. Commun.*, vol. E95-B, no. 3, pp. 991–994, 2012.

[23] D. Monderer and L. S. Shapley, "Potential games," *Games Econ. Behav.*, vol. 14, pp. 124–143, 1996.

[24] J. Marden and J. Shamma, "Game theory and distributed control," in *Handbook of Game Theory*, H. P. Young and S. Zamir, Eds. New York, NY, USA: Elsevier, 2012.

Achievable Rate of Rician Large-Scale MIMO Channels With Transceiver Hardware Impairments

Jiayi Zhang, Linglong Dai, Xinlin Zhang, Emil Björnson, and Zhaocheng Wang

***Abstract*—Transceiver hardware impairments (e.g., phase noise, in-phase/quadrature-phase imbalance, amplifier nonlinearities, and quantization errors) have obvious degradation effects on the performance of wireless communications. While prior works have improved our knowledge of the influence of hardware impairments of single-user multiple-input multiple-output (MIMO) systems over Rayleigh fading channels, an analysis encompassing the Rician fading channel is not yet available. In this paper, we pursue a detailed analysis of regular and large-scale (LS) MIMO systems over Rician fading channels by deriving new closed-form expressions for the achievable rate to provide several important insights for practical system design. More specifically, for regular MIMO systems with hardware impairments, there is always a finite achievable rate ceiling, which is irrespective of the transmit power and fading conditions. For LS-MIMO systems, it is interesting to find that the achievable rate loss depends on the Rician K-factor, which reveals that the favorable propagation in LS-MIMO systems can remove the influence of hardware impairments. However, we show that the nonideal LS-MIMO system can still achieve high spectral efficiency due to its huge degrees of freedom.**

***Index Terms*—Achievable rate, hardware impairments, large-scale (LS) multiple-input multiple-output (MIMO), Rician fading channels.**

I. Introduction

By employing multiple antennas at the transceiver, wireless systems can significantly increase spectral efficiency and transmission reliability. The capacity of single-user multiple-input multiple-output (MIMO) systems has been well investigated in the literature [1], [2]. However, most prior works assume that ideal hardware is available at both the transmitter and the receiver, which is unrealistic in practice, whereas the performance of practical MIMO systems is usually affected by transceiver hardware impairments, such as phase noise, in-phase/quadrature-phase imbalance, amplifier nonlinearities, and

Manuscript received June 3, 2015; revised October 10, 2015; accepted November 25, 2015. Date of publication December 1, 2015; date of current version October 13, 2016. This work was supported in part by the International Science and Technology Cooperation Program of China under Grant 2015DFG12760, by the National Natural Science Foundation of China under Grant 61571270 and Grant 61201185, and by the China Postdoctoral Science Foundation under Grant 2014M560081. The work of X. Zhang was supported in part by the Swedish Governmental Agency for Innovation Systems (VINNOVA) within the VINN Excellence Center Chase and the Swedish Foundation for Strategic Research. The work of E. Björnson was supported by the ELLIIT and the CENIIT project 15.01. The review of this paper was coordinated by Prof. D. B. da Costa.

J. Zhang is with the School of Electronics and Information Engineering, Beijing Jiaotong University, Beijing 100044, China (e-mail: jiayizhang@bjtu.edu.cn).

L. Dai, and Z. Wang are with the Department of Electronic Engineering and the Tsinghua National Laboratory of Information Science and Technology (TNList), Tsinghua University, Beijing 100084, China (e-mail: daill@tsinghua.edu.cn; zcwang@tsinghua.edu.cn).

X. Zhang is with the Department of Signals and Systems, Chalmers University of Technology, 412 96 Gothenburg, Sweden (e-mail: xinlin@chalmers.se).

E. Björnson is with the Department of Electrical Engineering (ISY), Linköping University, 581 83 Linköping, Sweden (e-mail: emil.bjornson@liu.se).

Color versions of one or more of the figures in this paper are available online at http://ieeexplore.ieee.org.

Digital Object Identifier 10.1109/TVT.2015.2504428

quantization errors [3]. Although the influence of these impairments can be mitigated by calibration methods and compensation schemes on both sides, there still remain residual hardware impairments due to estimation errors, inaccurate calibration methods, and different types of noise.

Recently, large-scale (LS) MIMO communication has drawn substantial interest from both academia and industry as a promising technology for fifth-generation wireless systems, such as millimeter-wave (mmWave) communications. LS-MIMO systems are likely to operate in the mmWave band to accommodate many antennas within a small physical area. In LS-MIMO systems, each base station is equipped with a large number of antennas to improve spectral and energy efficiency. Understanding the fundamental theoretical limits of the LS-MIMO system has been an active research area. For practical implementation, it is very attractive to deploy LS antenna elements with cheap, compact, and power-efficient radio and digital processing hardware. Thus, it is of profound importance to theoretically investigate how much hardware impairments can the LS-MIMO system tolerate to achieve a certain achievable rate performance.

Motivated by these observations, some researchers have analyzed the impact of transceiver hardware impairments on MIMO system performance. Specifically, experimental results to model the statistical behavior of residual hardware impairments on regular[1] MIMO systems have been provided in pioneering works such as those in [4] and [5]. Utilizing this impairment model, Björnson *et al.* in [6] and Zhang *et al.* in [7] analyzed the achievable rate of regular MIMO systems in detail. With the rapid development of LS-MIMO systems, people shift their interest to hardware impairments of LS-MIMO systems. In this context, the single type of impairments has been considered in [8]–[11] in terms of power amplifier nonlinearities, mismatched joint decoding, and phase noise. Moreover, in [3], [7], and [12], the achievable rate of LS-MIMO systems have been examined in detail by taking into account the effects of transceiver hardware impairments.

The common characteristic of the aforementioned works, however, is that they consider Rayleigh fading channels. Although the assumption of Rayleigh fading extensively simplifies the performance analysis, its validity is often violated in practical wireless propagation scenarios with the line-of-sight (LoS) path, where the Rician fading model is more general and accurate [13]. To the best of our knowledge, a detailed analysis of MIMO systems over Rician fading channels in the presence of transceiver hardware impairments is missing in the literature. Only recently has the high signal-to-noise ratio (SNR) capacity limit of regular MIMO systems over Rician fading channels been established in [6]. In this paper, we aim to fill this gap by investigating the impact of hardware impairments on the achievable rate of regular and LS-MIMO systems over Rician fading channels. Specifically, the contributions of this paper are summarized as follows.

- We derive a new analytical achievable rate expression for regular MIMO systems subject to Rician fading and hardware impairments. Although the expression is given in infinite series, the truncation error has been obtained to demonstrate its fast convergence. Additionally, we present asymptotic achievable rate expressions in the high-SNR regime, which coincide with the results in [6]. Moreover, based on our analysis, there is always a ceiling on the achievable rates of regular MIMO systems.
- For LS-MIMO systems, asymptotic expressions for the achievable rate are presented for three typical types of antenna arrays. Assuming perfect channel state information (CSI) at the receiver and no CSI at the transmitter, it is interesting to find that the achievable rate ceiling disappears by deploying a huge number of antennas at the transceiver. Moreover, our results show that the achievable rate gap between hardware impairments and perfect hardware increases with the value of the Rician K-factor.

The remainder of this paper is organized as follows: In Section II, the single-user MIMO channel model used throughout this paper is briefly introduced. Section III provides a detailed achievable rate analysis of MIMO systems with transceiver hardware impairments over Rician fading channels. A set of numerical results is given in Section IV. Finally, Section V concludes this paper.

II. System and Channel Model

We consider a single-user MIMO system with N_t transmit antennas and N_r receive antennas and assume that perfect CSI is available at the receiver, whereas no CSI can be obtained at the transmitter. The system model can be written as

$$\mathbf{y} = \mathbf{H}\mathbf{x} + \mathbf{n} \tag{1}$$

where $\mathbf{y} \in \mathbb{C}^{N_r \times 1}$ denotes the received signal vector; $\mathbf{x} \in \mathbb{C}^{N_t \times 1}$ is the transmitted signal vector with zero mean and covariance matrix $\mathtt{E}[\mathbf{x}\mathbf{x}^H] = \mathbf{Q}$, with $\mathtt{E}[\cdot]$ being the expectation operator and $(\cdot)^H$ being the Hermitian operation; and $\mathbf{n} \in \mathbb{C}^{N_r \times 1}$ denotes the vector of zero-mean complex circularly symmetric additive white Gaussian noise. Moreover, $\mathbf{H} \in \mathbb{C}^{N_r \times N_t}$ represents the Rician channel matrix modeling fast fading with a deterministic LoS path, which can be modeled as [14]

$$\mathbf{H} = \sqrt{\frac{K}{K+1}}\bar{\mathbf{H}} + \sqrt{\frac{1}{K+1}}\mathbf{H}_\omega \tag{2}$$

where $\bar{\mathbf{H}}$ denotes the deterministic component; $\mathbf{H}_\omega$ denotes the random fast-fading component, which is composed of independent and identically distributed circularly symmetric complex Gaussian random variables with zero mean and unit variance; and K is the Rician factor denoting the power ratio between $\bar{\mathbf{H}}$ and $\mathbf{H}_\omega$. In this paper, we normalize the channel matrix $\mathbf{H}$ as $\mathtt{E}[\mathtt{tr}(\mathbf{H}\mathbf{H}^H)] = N_r N_t$, where $\mathtt{tr}(\cdot)$ denotes the trace of a matrix.

In practical MIMO systems, the received signals will be unavoidably distorted by impairments of transceiver hardware components, such as filters, oscillators, converters, mixers, and amplifiers, in two different ways. First, the actually emitted signals are different from the desired signals at the transmitter due to transmitter hardware impairments [15]. Second, the received signals may suffer from distortion after the signal processing due to receiver hardware impairments. Although several signal compensation algorithms have been proposed and utilized at each antenna, there still remain some residual transceiver hardware impairments due to inaccurate modeling, imperfect CSI, errors in the estimation of impairments' parameters, and so forth [7].[2] Therefore, it is important to analyze the impact of transceiver hardware impairments on the performance of MIMO systems to provide useful guidance for practical systems design.

The aggregate transceiver hardware impairments can be approximated by independent additive distortion noise at both the transmitter and the receiver, which has been used and verified by experiments in many previous works [3], [7], [12]. Based on the system model (1), the actually received signal can be denoted as [12]

$$\mathbf{y} = \mathbf{H}(\mathbf{x} + \boldsymbol{\eta}_t) + \boldsymbol{\eta}_r + \mathbf{n} \tag{3}$$

[1]In contrast to the LS-MIMO system, we use the terminology regular MIMO for systems with a small number of antennas at the transmitter and the receiver, e.g., smaller than eight antennas.

[2]Among these residual transceiver hardware impairments, phase noise is probably the most severe factor in single-carrier transmission, whereas it is still not clear in multicarrier systems [3], [9], [10].

where the additive distortion noise terms $\boldsymbol{\eta}_t$ and $\boldsymbol{\eta}_r$ are ergodic stochastic processes that describe the hardware impairments at the transmitter and the receiver, respectively. This model is both analytically tractable and matches experimental results accurately. The experimental results have uncovered key characteristics that $\boldsymbol{\eta}_t$ and $\boldsymbol{\eta}_r$ follow Gaussian distribution with variance proportional to the average signal power [4], [5]. Moreover, $\boldsymbol{\eta}_t$ and $\boldsymbol{\eta}_r$ can be analytically approximated by the central limit theorem as $\boldsymbol{\eta}_t \sim \mathcal{CN}(0, \delta_t^2 \mathrm{diag}(q_1, \ldots, q_{N_t}))$ and $\boldsymbol{\eta}_r \sim \mathcal{CN}(0, \delta_r^2 \mathrm{tr}(\mathbf{Q})\mathbf{I}_{N_r})$ [12], where $q_1, q_2, \ldots, q_{N_t}$ are the diagonal elements of the signal covariance matrix $\mathbf{Q}$. Note that the new system model (3) is more general than the canonical model (1) and captures dominant practical characteristics of transceiver hardware impairments. The proportionality parameters δ_t and δ_r are related to the error vector magnitude (EVM) metric, which is widely used to quantify the mismatch between the expected signal and the actual signal in radio-frequency transceivers [16]. In practical wireless systems, such as long-term evolution, the EVM requirements are in the range $\delta_t \in [0.08, 0.175]$ [16]. Note that larger values of δ_t and δ_r indicate that the MIMO system experiences higher levels of impairments caused by inaccurate transceiver hardware components. Moreover, the case of $\delta_t = \delta_r = 0$ corresponds to ideal transceiver hardware components.

III. Achievable Rate

Here, we present a detailed achievable rate analysis of MIMO systems with transceiver hardware impairments over Rician fading channels. Recall that neither instantaneous nor statistical CSI is available at the transmitter but perfectly known at the receiver, we use equal power allocation on each transmit antenna as $\mathbf{Q} = (P/N_t)\mathbf{I}_{N_t}$ with the total transmit power P. Moreover, the average SNR per receive antenna is defined as $\rho = \mathbb{E}[\mathrm{tr}(\mathbf{Q})]/N_0$, where N_0 denotes the noise variance, which is normalized as $N_0 = 1$ in the following analysis. The new system model (3) considering hardware impairments can be written in the form of the canonical model (1) with noise variance, i.e.,

$$\boldsymbol{\Phi} \triangleq \begin{cases} \frac{\rho\delta_t^2}{N_t}\mathbf{H}^H\mathbf{H} + (\rho\delta_r^2 + 1)\,\mathbf{I}_{N_t}, & \text{if} \quad N_t < N_r \\ \frac{\rho\delta_t^2}{N_t}\mathbf{H}\mathbf{H}^H + (\rho\delta_r^2 + 1)\,\mathbf{I}_{N_r}, & \text{if} \quad N_t \geq N_r. \end{cases} \tag{4}$$

We further assume an ergodic channel where each codeword spans over an infinite number of realizations of the fading $\mathbf{H}$. Then, the ergodic achievable rate R can be expressed as [1]

$$R \triangleq \begin{cases} \mathbb{E}\left[\log_2 \det\left(\mathbf{I}_{N_t} + \frac{\rho}{N_t}\mathbf{H}^H\mathbf{H}\boldsymbol{\Phi}^{-1}\right)\right], & \text{if} \quad N_t < N_r \\ \mathbb{E}\left[\log_2 \det\left(\mathbf{I}_{N_r} + \frac{\rho}{N_t}\mathbf{H}\mathbf{H}^H\boldsymbol{\Phi}^{-1}\right)\right], & \text{if} \quad N_t \geq N_r. \end{cases} \tag{5}$$

A. Exact Analysis

For notational convenience, we define $p \triangleq \max(N_t, N_r)$, $q \triangleq \min(N_t, N_r)$, and the instantaneous MIMO channel correlation matrix $\mathbf{W}$ as

$$\mathbf{W} \triangleq \begin{cases} \mathbf{H}^H\mathbf{H}, & \text{if} \quad N_t < N_r \\ \mathbf{H}\mathbf{H}^H, & \text{if} \quad N_t \geq N_r. \end{cases} \tag{6}$$

Note that $\mathbf{W}$ is a complex noncentral Wishart matrix [17].

Lemma 1: The exact achievable rate of MIMO systems with residual hardware impairments over Rician fading channels can be expressed as

$$\begin{aligned} R = &\frac{G}{\ln(2)} \sum_{n=1}^{q} \sum_{m=1}^{q} D_{n,m} \sum_{k=0}^{\infty} \frac{\Gamma(p-q+m+k)\phi_n^k}{\Gamma(k+1)(p-q+1)_k} \\ &\times \sum_{t=1}^{p-q+m+k} \left(e^{\frac{(K+1)}{a}} E_{p-q+m+k-t+1}\left(\frac{K+1}{a}\right) \right. \\ &\left. - e^{\frac{(K+1)}{b}} E_{p-q+m+k-t+1}\left(\frac{K+1}{b}\right) \right) \end{aligned} \tag{7}$$

where $(x)_z \triangleq \Gamma(x+z)/\Gamma(x)$, $a \triangleq (\rho(1+\delta_t^2))/(N_t(1+\rho\delta_r^2))$, $b \triangleq \rho\delta_t^2/(N_t(1+\rho\delta_r^2))$, $E_z(x) = \int_1^\infty t^{-z}e^{-xt}dt$ is the exponential integral function [18, eq. (8.211.1)], $\boldsymbol{\phi} = [\phi_1, \phi_2, \ldots, \phi_q]^T$ is the squared singular values of $\sqrt{K}\bar{\mathbf{H}}$, and

$$G \triangleq \frac{\prod_{i=1}^{q} e^{-\phi_i}}{[(p-q)!]^q \prod\limits_{1 \leq i < j \leq q} (\phi_j - \phi_i)}. \tag{8}$$

Moreover, $D_{n,m}$ denotes the (n,m)th cofactor of the $(q \times q)$ matrix $\boldsymbol{\Omega}$, whose elements are given by

$$\boldsymbol{\Omega}_{n,m} = \Gamma(p-q+m)\,{}_1F_1(p-q+m, p-q+1, \phi_n) \tag{9}$$

where ${}_1F_1(\cdot)$ is the confluent hypergeometric function [18, eq. (9.21)].

Proof: The marginal probability density function of an unordered squared singular value of $\mathbf{W}$ is given by [19]

$$\begin{aligned} f(\lambda) = &\frac{Ge^{-\lambda(K+1)}}{q\lambda} \sum_{n=1}^{q} \sum_{m=1}^{q} D_{n,m}((K+1)\lambda)^{p-q+m} \\ &\times {}_0F_1\left(p-q+1; (K+1)\phi_n\lambda\right) \end{aligned} \tag{10}$$

where ${}_0F_1(\cdot)$ denotes the hypergeometric functions [18, eq. (9.14)] and can be expressed as ${}_0F_1(x,y) = \sum_{m=0}^{\infty}(y^m/(m!(x)_m))$ [20]. We can rewrite (5) as

$$\begin{aligned} R &= \frac{q}{\ln 2}\mathbb{E}\left[\ln\left(1 + \frac{\rho\lambda/N_t}{\rho\delta_t^2\lambda/N_t + \rho\delta_r^2 + 1}\right)\right] \\ &= \frac{q}{\ln 2}\left(\mathbb{E}\left[\ln(1+a\lambda)\right] - \mathbb{E}\left[\ln(1+b\lambda)\right]\right). \end{aligned} \tag{11}$$

By substituting (10) into (11), the first expectation of (11) can be derived as

$$\begin{aligned} \mathbb{E}\left[\ln(1+a\lambda)\right] &= \int_0^\infty \ln(1+a\lambda)\frac{Ge^{-\lambda(K+1)}}{q\lambda} \sum_{n=1}^{q}\sum_{m=1}^{q} D_{n,m} \\ &\quad \times {}_0F_1(p-q+1;(K+1)\phi_n\lambda)((K+1)\lambda)^{p-q+m}d\lambda \\ &= \frac{G}{q}\sum_{n=1}^{q}\sum_{m=1}^{q} D_{n,m} \sum_{k=0}^{\infty} \frac{\Gamma(p-q+m+k)\phi_n^k}{\Gamma(k+1)(p-q+1)_k} \\ &\quad \times \sum_{t=1}^{p-q+m+k} e^{\frac{(K+1)}{a}} E_{p-q+m+k-t+1}\left(\frac{K+1}{\alpha}\right) \end{aligned} \tag{12}$$

where we have used the following integral identity [19]:

$$\int_0^\infty \ln(1+\alpha x)\frac{x^{z-1}}{e^{\beta x}}dx = \frac{\Gamma(z)e^{\frac{\beta}{\alpha}}}{\beta^z}\sum_{l=1}^{z} E_{z-l+1}\left(\frac{\beta}{\alpha}\right). \tag{13}$$

The second expectation of (11) can be derived in a similar way. Then, the proof is ended by substituting the corresponding results [e.g., (12)] into (11). ■

TABLE I
REQUIRED TERMS OF SERIES T_0 TO ACHIEVE SATISFACTORY ACCURACY ($\leq 10^{-6}$)

ρ	N_t	N_r	δ_t	δ_r	K	T_0
0	2	2	0.15	0.15	1	11
0	2	2	0.15	0.15	5	15
10	2	2	0.15	0.15	1	10
0	4	4	0.15	0.15	1	12
0	2	2	0.1	0.1	1	12

To show the fast convergence of the infinite series in (7), we assume that only the $T_0 - 1$ first terms are used. Note that if $x < y$, the function $e^x E_n(x) - e^y E_n(y)$ is monotonically decreasing in n according to the derivative property of $E_n(x)$ [20, eq. (5.1.26)]. Then, the truncation error R_0 is upper bounded as (14), shown at the bottom of the page, where ${}_2F_2(\alpha_1, \alpha_2; \beta_1, \beta_2; z) = \sum_{k=0}^{\infty}((\alpha_1)_k(\alpha_2)_k/(\beta_1)_k(\beta_2)_k)(z^k/k!)$ is the generalized hypergeometric function [18, eq. (9.14.1)]. Moreover, the required terms of series T_0 have been investigated in Table I for different parameters. To achieve satisfactory accuracy, e.g., 10^{-6}, more terms are needed for larger values of K, N_t, and N_r. On the contrary, T_0 decreases with the larger values of SNR ρ. Finally, for all cases considered in Table I, only less than 15 terms need to be calculated.

B. High-SNR Analysis

Although (7) is the exact achievable rate, it provides little insight into how hardware impairments affect the achievable rate of MIMO systems over Rician fading channels. For high-SNR values, we can take $\rho \to \infty$ in (5) and follow a similar line of reasoning as in Lemma 1. Then, the asymptotic achievable rate approaches the finite limit, i.e.,

$$R^{\infty} = \frac{G}{\ln 2}\sum_{n=1}^{q}\sum_{m=1}^{q} D_{n,m}\sum_{k=0}^{\infty}\frac{\Gamma(p-q+m+k)\phi_n^k}{\Gamma(k+1)(p-q+1)_k} \times \sum_{t=1}^{p-q+m+k}\left(e^{\frac{(K+1)}{a'}}E_{p-q+m+k-t+1}\left(\frac{K+1}{a'}\right) - e^{\frac{(K+1)}{b'}}E_{p-q+m+k-t+1}\left(\frac{K+1}{b'}\right)\right) \quad (15)$$

where $a' \triangleq (1+\delta_t^2)/N_t\delta_r^2$ and $b' \triangleq \delta_t^2/N_t\delta_r^2$, respectively.

The term $(e^{(K+1)/a'}E_1((K+1)/a') - e^{(K+1)/b'}E_1((K+1)/b'))$ in (15) becomes zero when k is large [18]. Therefore, the achievable rate of MIMO systems over Rician fading channels with residual hardware impairments approaches a finite ceiling in the high-SNR regime, which is also found in the case of Rayleigh fading channels in [7] and the case of any fading channels with only transmitter impairments in [6]. This effect can be explained as that the transceiver distortion will increase with the transmit power. Accordingly, the equivalent SNR, i.e., $(\rho/N_t)\mathbf{H}\mathbf{H}^H\mathbf{\Phi}^{-1}$, in (5) will not increase. However, the achievable rate R will increase to infinity with SNR if adopting the ideal hardware. Moreover, (15) reveals that the residual hardware impairments dominate on the achievable rate performance of MIMO systems in the high-SNR regime.

Moreover, assuming that the first $T_0' - 1$ terms are used in the infinite series, the truncation error R_0' is upper bounded as

$$R_0' \leq \frac{\Gamma(p-q+m+T_0'+1)\,\phi_n^{T_0'}}{\Gamma(T_0'+1)\,(p-q+1)_{T_0'}} \times {}_2F_2(p-q+m+T_0'+1, 1; T_0'+1, p-q+T_0'+1; \phi_n) \times \left(e^{\frac{(K+1)}{a'}}E_1\left(\frac{K+1}{a'}\right) - e^{\frac{(K+1)}{b'}}E_1\left(\frac{K+1}{b'}\right)\right). \quad (16)$$

C. Asymptotic LS-MIMO Analysis

In the following, we consider the achievable rate of three-asymptotic-antenna deployment in LS-MIMO systems. Note that our analysis holds for any LoS model that satisfies the limit of $(1/p)\mathbf{H}\mathbf{H}^H \xrightarrow{a.s.} \mathbf{I}_q$. If a uniform linear array (ULA) is adopted at the transmitter, the (m,n)th entry $\bar{\mathbf{H}}_{mn}$ is given by

$$\bar{\mathbf{H}}_{mn} = e^{-j(m-1)\left(\frac{2\pi d}{\lambda}\right)\sin\theta_n} \quad (17)$$

where d is the transmit antenna spacing, λ is the wavelength, and θ_n is the arrival angle of the nth receive antenna. Moreover, we set $d = \lambda/2$, which means that there is no correlation between receive antennas.

First, the number of transmit antennas N_t tends to infinity, whereas the number of receiver antennas N_r is fixed. According to the law of large numbers, the correlation matrix $(1/N_t)\mathbf{H}\mathbf{H}^H - \mathbf{I}_{N_r} \xrightarrow{a.s.} \mathbf{0}$ [14, Lemma 2] as $N_t \to \infty$, where $a.s.$ denotes almost sure convergence. To take the limit inside the expectation in (5) by the dominated convergence theorem [21], the achievable rate reduces to

$$R_{N_t\to\infty} = N_r \log_2\left(1 + \frac{\rho}{\rho\delta_t^2 + \rho\delta_r^2 + 1}\right) \quad (18)$$

which indicates that the achievable rate of LS-MIMO systems with infinite N_t depends on the transceiver distortions, transmit SNR, and the number of receiver antennas N_r. Moreover, as we increase N_r,

$$\begin{aligned}
R_0 &= \sum_{k=T_0}^{\infty}\frac{\Gamma(p-q+m+k)\phi_n^k}{\Gamma(k+1)(p-q+1)_k}\sum_{t=1}^{p-q+m+k}\left(e^{\frac{(K+1)}{a}}E_{p-q+m+k-t+1}\left(\frac{K+1}{a}\right) - e^{\frac{(K+1)}{b}}E_{p-q+m+k-t+1}\left(\frac{K+1}{b}\right)\right)\\
&< \sum_{k=T_0}^{\infty}\frac{\Gamma(p-q+m+k+1)\phi_n^k}{\Gamma(k+1)(p-q+1)_k}\left(e^{\frac{(K+1)}{a}}E_1\left(\frac{K+1}{a}\right) - e^{\frac{(K+1)}{b}}E_1\left(\frac{K+1}{b}\right)\right)\\
&\overset{s=k-T_0}{=\!=} \frac{\Gamma(p-q+m+T_0+1)\phi_n^{T_0}}{\Gamma(T_0+1)\Gamma(p-q+T_0+1)}\sum_{s=0}^{\infty}\frac{(p-q+m+T_0+1)_s(1)_s}{(T_0+1)_s(p-q+T_0+1)_s}\frac{\phi_n^s}{s!}\left(e^{\frac{(K+1)}{a}}E_1\left(\frac{K+1}{a}\right) - e^{\frac{(K+1)}{b}}E_1\left(\frac{K+1}{b}\right)\right)\\
&= \frac{\Gamma(p-q+m+T_0+1)\phi_n^{T_0}}{\Gamma(T_0+1)(p-q+1)_{T_0}}\,{}_2F_2(p-q+m+T_0+1, 1; T_0+1, p-q+T_0+1; \phi_n)\\
&\quad\times\left(e^{\frac{(K+1)}{a}}E_1\left(\frac{K+1}{a}\right) - e^{\frac{(K+1)}{b}}E_1\left(\frac{K+1}{b}\right)\right) \qquad (14)
\end{aligned}$$

the achievable rate linearly grows. However, if N_r is fixed but the SNR is increased, the achievable rate asymptotically approaches the limit, as we have discussed in Section III-B. This fact suggests that the achievable rate will saturate in the high-SNR regime for Rician fading channels.

Then, we consider the second case, where the receiver employs a large number of receiver antennas N_r but the number of transmit antennas N_t is fixed. Recall that the ULA model is assumed and multiplying the term of $(\mathbf{I}_{N_t} + (\rho/N_t)\mathbf{H}^H\mathbf{H}\boldsymbol{\Phi}^{-1})$ in (5) by $1/N_r$, the achievable rate (5) can be written as

$$R = \mathbb{E}\left\{\log_2 \det\left(\mathbf{I}_{N_t} + \frac{\frac{\rho}{N_t N_r}\mathbf{H}^H\mathbf{H}}{\frac{\rho\delta_t^2}{N_t N_r}\mathbf{H}^H\mathbf{H} + \frac{(\rho\delta_r^2+1)}{N_r}\mathbf{I}_{N_t}}\right)\right\}. \quad (19)$$

As $N_r \to \infty$, we utilize the dominated convergence theorem and the fact that the noise term and the receiver distortion term go to zero. Then, (19) can approach

$$R_{N_r\to\infty} = N_t \log_2\left(1 + \frac{1}{\delta_t^2}\right). \quad (20)$$

It is clear that the achievable rate linearly grows with the number of transmit antennas N_t. Moreover, the receiver distortion (denoted by δ_r^2) and the SNR have no impact on the achievable rate performance. This shows the key difference from the first case of large N_t but fixed N_r, where both transceiver distortions (denoted by δ_t^2 and δ_r^2) characterize the system achievable rate performance. Such result suggests that employing low-cost hardware at the receiver is suitable if hardware impairments are unavoidable.

Finally, in the third case, large N_t and N_r and the general Rician fading model are considered, where the achievable rate R can be reexpressed as

$$\begin{aligned} R &= \mathbb{E}\left[\log_2 \det\left(\frac{\rho(1+\delta_t^2)}{N_t}\mathbf{H}\mathbf{H}^H + (\rho\delta_r^2+1)\mathbf{I}_{N_r}\right)\right. \\ &\qquad \left. - \log_2 \det\left(\frac{\rho\delta_t^2}{N_t}\mathbf{H}\mathbf{H}^H + (\rho\delta_r^2+1)\mathbf{I}_{N_r}\right)\right] \\ &= \mathbb{E}\left[\log_2 \det(a\mathbf{H}\mathbf{H}^H + \mathbf{I}_{N_r}) + N_r \log_2(\rho\delta_r^2+1)\right. \\ &\qquad \left. - \log_2 \det(b\mathbf{H}\mathbf{H}^H + \mathbf{I}_{N_r}) - N_r\log_2(\rho\delta_r^2+1)\right] \\ &= \mathbb{E}\left[\log_2 \det(a\mathbf{H}\mathbf{H}^H + \mathbf{I}_{N_r}) - \log_2\det(b\mathbf{H}\mathbf{H}^H + \mathbf{I}_{N_r})\right] \\ &= J\left(\frac{1}{a}, \mathbf{I}_{N_r}\right) - J\left(\frac{1}{b}, \mathbf{I}_{N_r}\right) \end{aligned} \quad (21)$$

where $J(1/a, \mathbf{I}_{N_r}) \triangleq E[\log_2 \det(a\mathbf{H}\mathbf{H}^H + \mathbf{I}_{N_r})]$, and $J(1/b, \mathbf{I}_{N_r}) \triangleq E[\log_2 \det(b\mathbf{H}\mathbf{H}^H + \mathbf{I}_{N_r})]$, respectively. From [21, Th. 6.14], we have a large-system approximation of the achievable rate $J(1/a, \mathbf{I}_{N_r})$ for a large number of antennas at both the transmitter and receiver sides $(N_t, N_r \to \infty)$ and uniform transmit power allocation as [21, eq. (13.10)]

$$J\left(\frac{1}{a}, \mathbf{I}_{N_r}\right) - \left[\log_2 \det(a\boldsymbol{\Psi}^{-1} + \bar{\mathbf{H}}\bar{\boldsymbol{\Psi}}\bar{\mathbf{H}}^T) + \log_2\det(a\boldsymbol{\Psi}^{-1})\right. \\ \left. - \frac{\log_2(e)}{aN_t}\sum_{i,j}\frac{v_i\bar{v}_j}{K+1}\right] \xrightarrow{a.s.} 0 \quad (22)$$

where $\boldsymbol{\Psi}$ denotes the diagonal matrix with the ith entry ψ_i, and $\bar{\boldsymbol{\Psi}}$ is the diagonal matrix with the jth entry $\bar{\psi}_j$, respectively. Moreover, we define v_i and $\bar{v}_j$ as the ith diagonal entry of $(\bar{\boldsymbol{\Psi}}^{-1} + (1/a)\bar{\mathbf{H}}^T\boldsymbol{\Psi}\bar{\boldsymbol{H}})^{-1}$ and the jth diagonal entry of $(\boldsymbol{\Psi}^{-1} + (1/a)\bar{\mathbf{H}}\bar{\boldsymbol{\Psi}}\bar{\mathbf{H}}^T)^{-1}$, respectively. As $N_t \to \infty$, the error between the right-hand side of (22) goes almost surely to zero. It is clear from (22) that the approximation error asymptotically decreases by increasing the number of transmit antennas N_t. The entries ψ_i and $\bar{\psi}_j$ can be obtained by solving

$$\begin{cases} \psi = a\left[1 + \frac{1}{N_t(K+1)}\mathrm{tr}\left\{\left(\frac{1}{\bar{\psi}}\mathbf{I}_{N_t} + \frac{\psi}{a}\bar{\mathbf{H}}^T\bar{\mathbf{H}}\right)^{-1}\right\}\right]^{-1} \\ \bar{\psi} = a\left[1 + \frac{1}{N_t(K+1)}\mathrm{tr}\left\{\left(\frac{1}{\psi}\mathbf{I}_{N_r} + \frac{\bar{\psi}}{a}\bar{\mathbf{H}}\bar{\mathbf{H}}^T\right)^{-1}\right\}\right]^{-1}. \end{cases} \quad (23)$$

Note that the equations in (23) are fixed-point iterations. The unknown variables ψ and $\bar{\psi}$ can be easily obtained by solving the formulas in (23). Substituting ψ and $\bar{\psi}$ into (22) and using the similar method to calculate $J(1/b, \mathbf{I}_{N_r})$, the desired achievable rate in (21) can be derived.

IV. Numerical Results

Here, we illustrate the key analytical insights presented in Section III by various Monte Carlo simulations. For the ideal and nonideal systems, the achievable rate results have been obtained by means of Monte Carlo simulations using 10^6 trails, respectively. Furthermore, the LoS model in (17) has been used in our simulations.

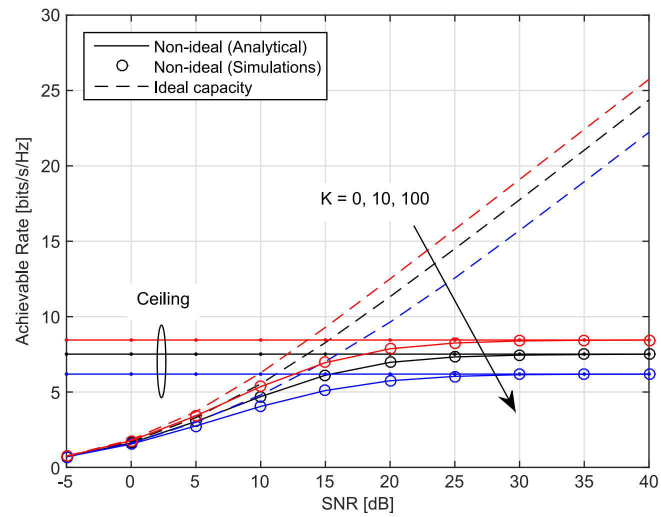

Fig. 1. Achievable rate of regular MIMO systems with hardware impairments against SNR and Rician K-factor, where $\delta_t = \delta_r = 0.15$ and $N_t = N_r = 2$.

In Fig. 1, the simulated achievable rate, the analytical result (7), and the high-SNR approximation (15) of regular MIMO systems with hardware impairments are plotted against the SNR and Rician K-factor, where $\delta_t = \delta_r = 0.15$ and $N_t = N_r = 2$ are considered. Fig. 1 validates the accuracy of our derived analytical expressions in (7) and (15). For the case of hardware impairments, it is clear that there is a finite rate ceiling, which cannot be crossed by increasing the SNR value. Furthermore, we observe that an increase in SNR tends to increase the achievable rate of both the ideal and nonideal systems, albeit the relative difference between the curves gets steadily larger. In addition, a higher K value yields a lower achievable rate, although the gap between the corresponding curves decreases as K increases, which implies that its effect becomes less pronounced.

The achievable rate of single-user LS-MIMO systems with ideal and nonideal hardware is shown in Fig. 2, which reveals that the

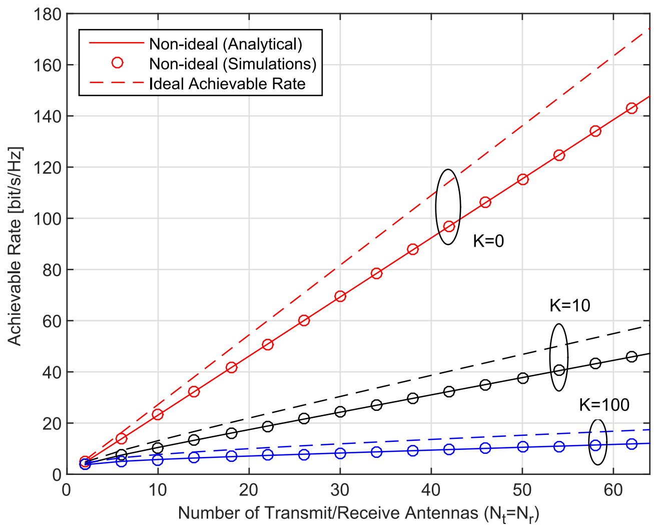

Fig. 2. Achievable rate of LS-MIMO systems with hardware impairments against the number of transmit and receive antennas and Rician K-factor, where $\delta_t = \delta_r = 0.15$, $\rho = 10$ dB, and $N_t = N_r$.

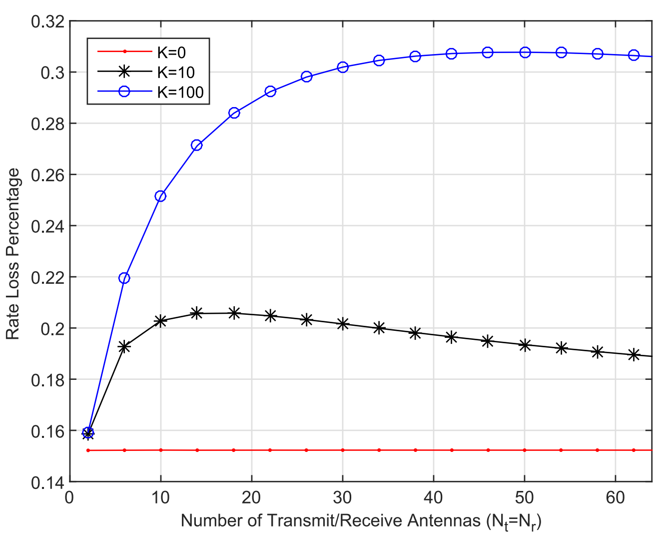

Fig. 3. Achievable rate loss of LS-MIMO systems with hardware impairments against the number of transmit antennas N_t and Rician K-factor, where $\delta_t = \delta_r = 0.15$, $\rho = 10$ dB, and $N_t = N_r$.

finite achievable rate ceiling disappears for large numbers of transmit and receive antennas. This phenomenon is consistent with the results with Rayleigh fading channels in [7]. This is because the reduction in effective SNR, i.e., ρ/N_t, can be compensated by the large array gain at the receiver. As expected, the increased LoS component (larger values of K) will decrease the rank of the correlation matrix and the system's achievable rate.

To further investigate the effect of the Rician K-factor on the achievable rate of LS-MIMO systems, we introduce a new metric as $R_{\mathrm{loss}} = (R_{\mathrm{ideal}} - R_{\mathrm{nonideal}})/R_{\mathrm{ideal}}$, which denotes the achievable rate loss between ideal and nonideal systems with hardware impairments. Moreover, we assume that the number of transmit and receive antennas grows together. It is important to observe from Fig. 3 that the achievable rate loss R_{loss} increases with the value of the Rician K-factor. However, with a relatively large number of antennas at both the transmitter and receiver sides, the achievable rate loss approaches a finite value. For example, the relative achievable rate loss R_{loss} for $K = 0$ is around 15%, whereas $R_{\mathrm{loss}} \to 30.5\%$ for the case of $K = 100$. Therefore, it is more important to utilize ideal hardware at LS-MIMO systems when operating over strong LoS environment.

V. Conclusion

In this paper, we have presented a detailed achievable rate analysis of regular and LS-MIMO systems under transceiver hardware impairments and Rician fading conditions. New analytical achievable rate results are derived for finite and infinite numbers of transceiver antennas. We obtain an asymptotic high-SNR achievable rate expression to reveal a finite ceiling in regular MIMO systems. Moreover, the impact of the Rician K-factor and hardware impairments on the achievable rate performance are investigated. Our findings reveal that the achievable rate ceiling vanishes by increasing both the number of transmit and receive antennas in LS-MIMO systems. Finally, we conclude that the achievable rate loss due to hardware impairments increases with the value of the Rician K-factor.

References

[1] E. Telatar, "Capacity of multi-antenna Gaussian channels," *Eur. Trans. Telecommun.*, vol. 10, no. 6, pp. 585–595, 1999.

[2] J. Zhang, L. Dai, Y. Han, Y. Zhang, and Z. Wang, "On the ergodic capacity of MIMO free-space optical systems over turbulence channels," *IEEE J. Sel. Areas Commun.*, vol. 33, no. 9, pp. 1925–1934, Sep. 2015.

[3] E. Björnson, M. Matthaiou, and M. Debbah, "Massive MIMO with arbitrary non-ideal arrays: Hardware scaling laws and circuit-aware design," *IEEE Trans. Wireless Commun.*, vol. 14, no. 8, pp. 4353–4368, Aug. 2015.

[4] C. Studer, M. Wenk, and A. Burg, "MIMO transmission with residual transmit-RF impairments," in *Proc. ITG/IEEE WSA*, Feb. 2010, pp. 189–196.

[5] C. Studer, M. Wenk, and A. Burg, "System-level implications of residual transmit-RF impairments in MIMO systems," in *Proc. IEEE EuCAP*, Apr. 2011, pp. 2686–2689.

[6] E. Björnson, P. Zetterberg, M. Bengtsson, and B. Ottersten, "Capacity limits and multiplexing gains of MIMO channels with transceiver impairments," *IEEE Commun. Lett.*, vol. 17, no. 1, pp. 91–94, Jan. 2013.

[7] X. Zhang, M. Matthaiou, E. Björnson, M. Coldrey, and M. Debbah, "On the MIMO capacity with residual transceiver hardware impairments," in *Proc. IEEE ICC*, Jun. 2014, pp. 5299–5305.

[8] S. K. Mohammed and E. G. Larsson, "Per-antenna constant envelope precoding for large multi-user MIMO systems," *IEEE Trans. Commun.*, vol. 61, no. 3, pp. 1059–1071, Mar. 2013.

[9] A. Pitarokoilis, S. Mohammed, and E. G. Larsson, "Uplink performance of time-reversal MRC in massive MIMO systems subject to phase noise," *IEEE Trans. Wireless Commun.*, vol. 14, no. 2, pp. 711–723, Feb. 2015.

[10] R. Krishnan *et al.*, "Linear massive MIMO precoders in the presence of phase noise—A large-scale analysis," *IEEE Trans. Veh. Technol.*, vol. 65, no. 5, pp. 3057–3071, May 2016.

[11] M. Vehkapera *et al.*, "Asymptotic analysis of SU-MIMO channels with transmitter noise and mismatched joint decoding," *IEEE Trans. Commun.*, vol. 63, no. 3, pp. 749–765, Mar. 2015.

[12] E. Björnson, J. Hoydis, M. Kountouris, and M. Debbah, "Massive MIMO systems with non-ideal hardware: Energy efficiency, estimation, and capacity limits," *IEEE Trans. Inf. Theory*, vol. 60, no. 11, pp. 7112–7139, Nov. 2014.

[13] J. Brady, N. Behdad, and A. M. Sayeed, "Beamspace MIMO for millimeter-wave communications: System architecture, modeling, analysis, and measurements," *IEEE Trans. Antennas Propag.*, vol. 61, no. 7, pp. 3814–3827, Jul. 2013.

[14] Q. Zhang, S. Jin, K.-K. Wong, H. Zhu, and M. Matthaiou, "Power scaling of uplink massive MIMO systems with arbitrary-rank channel means," *IEEE J. Sel. Topics Signal Process.*, vol. 8, no. 5, pp. 966–981, Oct. 2014.

[15] X. Dai, R. Zou, S. Sun, and Y. Wang, "Transceiver impairments on the performance of the LMMSE-PIC iterative receiver and its mitigation," *IEEE Commun. Lett.*, vol. 17, no. 8, pp. 1536–1539, Aug. 2013.

[16] H. Holma and A. Toskala, *LTE for UMTS: Evolution to LTE-Advanced*. Chichester, U.K.: Wiley, 2011.

[17] A. Zanella, M. Chiani, and M. Z. Win, "On the marginal distribution of the eigenvalues of Wishart matrices," *IEEE Trans. Commun.*, vol. 57, no. 4, pp. 1050–1060, Apr. 2009.
[18] I. S. Gradshteyn and I. M. Ryzhik, *Table of Integrals, Series, and Products*, 7th ed. San Diego, CA, USA: Academic, 2007.
[19] G. Alfano, A. Lozano, A. M. Tulino, and S. Verdú, "Mutual information and eigenvalue distribution of MIMO Ricean channels," in *Proc. IEEE ISITA*, Oct. 2004, pp. 1–6.
[20] M. Abramowitz and I. A. Stegun, *Handbook of Mathematical Functions with Formulas, Graphs, and Mathematical Tables*, 9th ed. New York, NY, USA: Dover, 1964.
[21] R. Couillet and M. Debbah, *Random Matrix Methods for Wireless Communications*. Cambridge, MA, USA: Cambridge Univ. Press, 2011.

Stable A/G MIMO Transmission Aided by Open-Loop Calibrated Channel Estimation and Adaptive Precoding

Chao Zhang, *Member, IEEE*, Lu Ma, and Keke Pang

***Abstract*—Due to the high flight speed of the aircraft and long range to access the ground station (GS), the channel state information (CSI) is not accurately obtained by direct feedback from the receiver to the transmitter. This makes it difficult to achieve stable transmission when the feedback codebook selection scheme is directly employed in the multiple-input multiple-output (MIMO) for the air-to-ground (A/G) communications. Therefore, in this paper, a stable transmission scheme for the A/G MIMO transmission is proposed to handle these issues. Two contributions are proposed: 1) an open-loop calibrated channel estimation scheme based on navigation filtering to offer a more accurate CSI estimation; and 2) an adaptive precoding scheme based on the correlation coefficient for stable transmission. The simulations confirm the validity and efficiency of the proposed schemes. For the 4 $\times$ 4 MIMO transmission, compared with the traditional scheme of a single antenna, the spectrum efficiency can be improved by 2 $\sim$ 4 times with a stable transmission.**

***Index Terms*—Air-to-ground (A/G) communications, codebook selection, multiple-input multiple-output (MIMO), navigation, open loop, precoding, stable transmission.**

I. Introduction

Multiple-input multiple-output (MIMO) is a promising technology for wireless broadband communications to resolve the contradiction between the channel capacity requirement and the limited frequency spectrum resource. For air-to-ground (A/G) communications, MIMO can also be employed to establish broadband MIMO communications [1]. However, the available channel capacity varies greatly with the distance between the aircraft and the ground station (GS), as indicated in [2]. In other words, the variance of the channel capacity is large due to the correlation among the MIMO channels. For the terrestrial mobile communications, a Long-Term Evolution (LTE) system provides a stable MIMO transmission based on codebook selection to overcome the channel variation [3], i.e., the receiver estimates the MIMO channel and selects the optimal codebook for the feedback. However, this scheme is not suitable for A/G communications due to the following two major reasons:

1) A huge cell in the A/G communications, usually with the radius of about 300 km, leads to a nonignorable delay of 2 ms from the feedback, when the aircraft flies on the edge of the cell [4]. However, the symbol period is fewer than several hundred microseconds (μs), i.e., the delay is much longer.
2) The high speed of the aircraft, usually about 1000 km/h, leads to the very fast variation of the MIMO channel. For example, if the communication in the L-band is undertaken, the Doppler spread reaches up to 1.8 kHz, which results in coherence time of about 0.54 ms. In other words, the channel can be considered as constant only within 0.54 ms. Indubitably, it is a harsh limitation for the A/G MIMO communications [5].

Taking the civil aviation scenario into consideration, the Rician channel model referred in [6] is employed in this paper, where the flights with a maximum speed of 440 m/s and at a maximum height of 10 km are considered. Although the Rician model in [6] is proposed for the single-input–single-output (SISO) channel, the A/G MIMO channel measurements carried out in [7] and [8] reveal that the line-of-sight (LOS) component and the multipath component coexist in the channel, i.e., the channel is a Rician model. Meanwhile, the Rician model is always employed to analyze the performance of the A/G MIMO transmission as indicated by [1], [2], and [9]. To be rigorous, the parameter of the stationary distance (SD) reported in [10], in which the channel is wide sense stationary, can also be taken into account in the A/G communications. Although this does not reduce the contributions of this paper, due to space limitations, the SD parameter will be discussed in the future.

Usually, the LOS MIMO system is applied in the quasi-static transmission rather than in mobile communications, because the fixed relative displacement between the transmitter and the receiver is the necessary condition to optimize the interelement spacing of the antennas in terms of the transmission capacity [11]. Some relevant discussions can be referred in [12] and [13]. However, such relative displacement is variant in the A/G MIMO communications, which makes optimization difficult. Specifically, if a stable A/G MIMO transmission is expected, at least two difficulties should be overcome. First, accurate channel state information (CSI) should be estimated and tracked during the flight. Second, a suitable codebook selection scheme is expected to perform adaptive precoding.

In this paper, different from the traditional MIMO schemes [14], [15], an open-loop calibrated channel estimation filtered by the navigation information is proposed to obtain more accurate CSI. Moreover, based on this CSI, the correlation coefficient is calculated, and an adaptive space–time coding scheme is proposed. The remainder of this paper is organized as follows. Section II shows the system architecture of the A/G MIMO transmission. Section III proposes the filtering scheme with the navigation information for the accurate CSI estimation. Section IV shows the adaptive precoding scheme. Section V evaluates the performance with simulations. Section VI presents some discussion, and the conclusion is drawn in Section VII.

II. System Architecture

The A/G channel contains a strong LOS component, indicated by a typical Rician model with a high K factor, which can be written as

$$\mathbf{H} = \sqrt{\frac{K}{K+1}}\mathbf{H}_{\mathrm{LOS}} + \sqrt{\frac{1}{K+1}}\mathbf{H}_{\mathrm{NLOS}} \tag{1}$$

Manuscript received March 13, 2015; revised October 10, 2015, December 7, 2015; accepted December 13, 2015. Date of publication December 24, 2015; date of current version October 13, 2016. This work was supported by the National 973 Project in China under Grant 2014CB744900. The review of this paper was coordinated by Dr. C. Yuen.

The authors are with the Laboratory of Avionics, School of Aerospace Engineering, Tsinghua University, Beijing 100084, China (e-mail: zhangchao@tsinghua.edu.cn).

Color versions of one or more of the figures in this paper are available online at http://ieeexplore.ieee.org.

Digital Object Identifier 10.1109/TVT.2015.2512299